PHYSICAL REVIEW B **69**, 024302 (2004)

First-principles study of hydrogen diffusion in α-Al_2O_3 and liquid alumina

A. B. Belonoshko,[1,*] A. Rosengren,[1] Q. Dong,[2] G. Hultquist,[2] and C. Leygraf[2]
[1]*Condensed Matter Theory, AlbaNova University Center, The Royal Institute of Technology, SE-106 91 Stockholm, Sweden*
[2]*Division of Corrosion Science, The Royal Institute of Technology, SE-100 44 Stockholm, Sweden*

(Received 29 May 2003; revised manuscript received 21 October 2003; published 21 January 2004)

We have studied the energetics and mobility of neutral hydrogen in alumina Al_2O_3 using *ab initio* density-functional calculations. The mobility of hydrogen was studied in corundum (α-Al_2O_3) as well as in liquid alumina. Using both static as well as molecular-dynamics calculations, and applying classical transition state theory, we derive the temperature-dependent diffusivity of hydrogen in α-Al_2O_3 as $D(T)=(21.7\times10^{-8}\ \mathrm{m^2/s})\exp(-1.24\ \mathrm{eV}/kT)$. The corresponding diffusivity of hydrogen in liquid/amorphous alumina, derived directly from *ab initio* molecular dynamics calculations, is $D(T)=(8.71\times10^{-7}\ \mathrm{m^2/s})\exp(-0.91\ \mathrm{eV}/kT)$. The computed diffusivity compares very well to experimental data. We conclude that diffusion of neutral hydrogen through the bulk of alumina is a good approximation of the mechanism for hydrogen mobility in corrosion scales. The representation of grain-boundary structures by amorphous alumina is, probably, realistic at higher temperatures.

DOI: 10.1103/PhysRevB.69.024302 PACS number(s): 66.30.Jt, 66.10.−x, 81.65.Kn, 71.15.Pd

I. INTRODUCTION

Hydrogen in its various chemical forms (atomic, ionic, or molecular) is known to have a profound influence on various forms of corrosion. At low or medium temperature there is clear evidence that protons promote the dissolution of metal oxides or minerals through ligand-induced metal dissolution.[1] In the presence of anions, protons, hydroxyl ions, or other ligands, surface chelates are formed that may weaken the metal-oxygen bonds and thereby promote the metal dissolution rate. At high-temperature hydrogen entry into bulk metals or alloys may result in hydrogen embrittlement or hydrogen-induced cracking, a most detrimental form of corrosion.[2] Various forms of hydrogen may also enter into metal oxides at high temperature and influence their defect structure, thereby altering the conditions for transport of species through the oxide.[3] While a natural source for hydrogen is water vapor, the identification of the chemical form of hydrogen in high-temperature oxides may be far from obvious.[4,5] Another source for hydrogen in high-temperature oxides on metallic materials is the metal itself from which hydrogen can migrate into the oxide and induce increased metal cation mobility.[6] However, the presence of hydrogen is not always detrimental. With the aim of forming dense barrier layers of metal oxides an addition of hydrogen to the oxide can be beneficial. This is due to an improved balance between anion and cation mobility[6] which is a prerequisite for a self-repairing metal oxide grown on a metallic substrate. The particular form of hydrogen which enters a corrosion scale is uncertain. However, we know that the hydrogen molecule dissociates at a surface of metal[7] and then enters the metal in atomic form.[2] If the concentration of hydrogen in the metal is small, then recombination of hydrogen can be neglected. This atomic hydrogen then enters the adjacent corrosion scale.

To understand the role of hydrogen in corrosion scales, one has to be able to estimate its mobility. We have chosen alumina (Al_2O_3) as a representative oxide to study diffusion of hydrogen. Alumina has a large number of different crystallographic polymorphs.[8–10] At ambient conditions, the stable alumina polymorph is α-Al_2O_3, known as corundum. The α-Al_2O_3 crystal structure can be described as follows. It is composed of six oxygen planes in the hcp ($ABAB\ldots$) stacking sequence,[11] where the Al cations occupy two-thirds of the octahedral interstitial sites.

Various phases of alumina[12–15] and hydrogen[16] have been carefully studied both experimentally and theoretically. This interest is well justified from a fundamental as well as an applied point of view. A number of models were developed to describe the interaction between the constituting atoms.[17–19] However, to the authors knowledge, there are no semiempirical models which are capable of describing interactions between hydrogen and alumina atoms. In this situation, a nonempirical method is the only choice.

Diffusion in a bulk material can occur via a comparatively ideal crystal structure as well as via extended defects, the largest of them being a grain-boundary. In this work, relying to a large extent on first-principle based simulations, we first estimate the diffusion in a perfect α-Al_2O_3 crystal. Then, after making various assumptions regarding the grain boundary structure in alumina, we approximate this structure by an amorphous structure. By conducting *ab initio* molecular dynamics (MD) simulations at several temperatures, we can derive the diffusivity by fitting our simulated data for these temperatures to a general expression for diffusivity.

The paper is organized as follows. In the following section, we describe our method and its verification. Then, in Sec. III, we describe the application of the method and the results obtained for hydrogen diffusivity. By comparing the calculated results on diffusivity to experimental data, we discuss their applicability to alumina with different morphology and summarize the obtained results.

II. METHOD

In our study for total energy and *ab initio* MD calculations we use the Vienna *Ab initio* Simulation Package

(VASP).[20–23] Our calculations are based on the full-potential frozen-core all-electron projected augmented wave (PAW) method [as implemented in VASP (Ref. 23)]. The energy cutoff was set to 500.0 eV. Exchange and correlation effects were treated in the framework of the generalized gradient approximation of Perdew and co-workers,[25] usually referred to as PW91. The integration over the Brillouin zone was performed using the Γ point as well as k points determined according to the Monkhorst-Pack scheme.[24] We tested our method by performing calculations on α-Al_2O_3. As initial configuration we have chosen the experimental hexagonal structure[26] with $a=b=4.656$ Å and $c=13.140$ Å. After relaxing the structure (forces on atoms are smaller than 10^{-4} eV/Å) we obtained the hexagonal cell with the parameters $a=b=4.781$ Å and $c=13.092$ Å. The resulting pressure was equal to 0.08 kbar. As another test of our method we calculated the relaxation of the 0001 α-Al_2O_3 surface and obtained very good agreement with experimental[27] and previously calculated[28] data on the relaxation of oxygen layers. The relaxation of the aluminum atoms at the surface of corundum in the oxygen plane was also reproduced. The ability of our method to get a good description of the hydrogen molecule was previously demonstrated.[30] Having tested our method and obtaining very reasonable results, we attempted to directly simulate the motion of a hydrogen atom inside the α-Al_2O_3 structure, but quickly recognized that even at considerable temperatures (comparable to the melting temperature T_m) in the simulation even a single jump of an hydrogen atom between energy minima positions would be a rare event. Therefore, in our calculations of hydrogen diffusion we instead employed an approximate expression, based on classical transition state theory:

$$D(T)=l^2\nu\exp\left(-\frac{E_a}{kT}\right), \tag{1}$$

where l is the hopping distance between energy minima, ν is the attempt frequency, E_a is the activation barrier, k is the Boltzmann constant, and T is the temperature.

Since T is the external parameter and l is provided by the crystal geometry, we need first to calculate E_a, which is the difference between the energies of the cell when hydrogen is located at the most energetically favorable position and when hydrogen is located at the saddle point connecting the two energy minima positions. Further we have to calculate as well ν, the attempt frequency.

Apart from the diffusion of hydrogen through the bulk alumina, diffusion might (and probably does) occur via the largest defects, grain boundaries (GB). A simulation of the environment in which hydrogen diffuses in this case represents a difficult problem for two reasons. First, there are basically no experimental data on the structure of GB in alumina, particularly at high temperature. Even the structure of alumina surfaces except for the 0001 surface[27] is not known.

A grain boundary represents an environment, where the symmetry of a crystal is terminated, that is, it is boundary between two cuts of crystal structure. Obviously, the atoms at this boundary have higher energy compared to the ideal crystal structure. Therefore, to destroy the symmetry at the surfaces one need to heat them to temperatures which are lower than the bulk melting temperature. Premelting of surfaces is a well-known phenomena. For example, in simulations of chromia with corundum structure it was observed that a slab of Cr_2O_3 melts at temperatures considerably below bulk melting temperatures.[29] Therefore, the approximation of a grain boundary by liquid at high temperature seems to be reasonable.

To check this, we applied molecular dynamics using the well tested[12–15] pairwise model.[17,18] This model is simple and has demonstrated its capacity to reproduce a number of experimental properties such as structure of various polymorphs, density, bulk modulus, thermal expansion,[18] melting temperature, pressure dependence of the melting temperature, and liquid structure among others. The potential employs pairwise additive interatomic terms of the forms

$$V(r_{ij})=\frac{q_iq_j}{r_{ij}}-\frac{C_iC_j}{r_{ij}^6}+D(B_i+B_j)\exp\left(\frac{A_i+A_j-r_{ij}}{B_i+B_j}\right), \tag{2}$$

where the individual terms represent Coulomb, van der Waals, and repulsion energy, respectively. Here r_{ij} is the distance between atoms i and j, and D is a standard force constant equal to 4.184 kJ/Å mol. The parameters A_i, B_i, and C_i are provided elsewhere.[17] The initial configuration used was two crystal (α-Al_2O_3) fragments embedded in presimulated liquid alumina. Periodic boundary conditions have been applied. Simulations have been performed at constant pressure[31] and temperature.[32] However, even very long MD simulation runs did show that the molten alumina in between the crystal fragments did not crystallize in the corundum structure. Therefore, we concluded that the GB structure may be approximated by amorphous alumina.

III. RESULTS AND DISCUSSION

The activation energy barrier (E_a) was determined as the difference between the energy minimum and the energy of the saddle point. A common condition for both minimum and saddle points are that the forces acting on the hydrogen atom are zero. The minimum point was found by relaxation of the hydrogen atom coordinates. Two possibilities have been considered, namely (1) H atom occupies an empty interstitial and (2) H occupies the interstitial which already contains an Al atom. The latter was found quite unfavorable. Since these two possibilities are the only ones, the found minimum-energy position of H is a global energy minimum. The hydrogen minimum position represents an empty interstitial in between the close-packed O layers. This interstitial is surrounded by the interstitials filled with Al atoms. Therefore, diffusion in between the O layers is energetically quite unfavorable. To jump to another minima position, the H atom has to cross the O layer. Since positions of empty interstitials possess a screw symmetry, the diffusion of H occurs along the c axis simultaneously moving around it. The saddle point was found from symmetry consideration as well as by the nudge elastic band method using eight images. Both methods

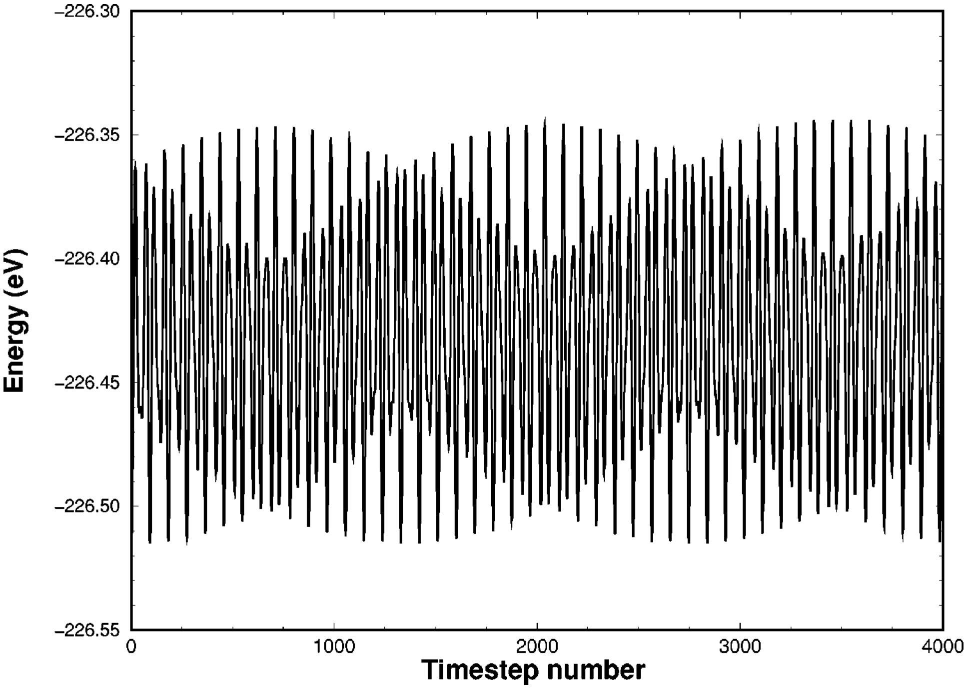

FIG. 1. Total potential energy of the α-Al_2O_3+H system (12 Al, 18 O, and 1 H atoms) as a function of time (1 time step $=0.5$ fs). Al and O atoms are fixed. The hydrogen atom moves with the initial kinetic energy corresponding to 1300 K.

resulted in identical saddle-point position and energy. The saddle point is located in the O layer at the point equidistant from O atoms. The check for the saddle point was that (1) forces are zero and (2) any infinitesimal change of hydrogen initial coordinates leads to a finite change of atomic coordinates. Subtracting these energies we obtained the activation energy to be 1.24 eV. To ensure that this value is independent of the chosen simulation cell and the integration over the Brillouin zone, we performed tests with the k-point grid of $2\times2\times2$ and $4\times4\times4$ as well as with the cell where the lateral size was doubled. The activation energy barrier E_a was in these cases equal to 1.42 eV, 1.36 eV, and 1.32 eV, respectively. All these values were obtained with all atoms relaxed before placing hydrogen in the minimum or saddle point. When atoms are relaxed with the hydrogen inside the cell, the activation energy barrier becomes equal to 1.10 eV. This is mainly due to comparably large relaxation at the saddle point. The relaxation at the minimum point is small. Given that the scatter of experimental data for E_a is large, ranging from -0.8 to -3.0 eV, we believe that the precision of our calculations is sufficient. Because we could not for technical reasons do any MD calculations with many k points, we for the purpose of consistency use the value 1.24 eV for the activation energy barrier.

The attempt frequency ν was calculated by placing one hydrogen atom in the potential energy minimum and providing this hydrogen atom with a kinetic energy corresponding to 1300 K while keeping the Al and O atoms fixed. The time step for solving the equations of motion is 0.5 fs (1 fs $=10^{-15}$ s). The calculated total potential energy of the system is shown in Fig. 1. One can see that there are several frequencies present. Since the attempt is the event to approach the saddle-point energy, we consider ν equal to the frequency of the peaks with the highest energy in Fig. 1. The high-frequency oscillations correspond to the attempts to move in the direction with high-energy gradient, while the low-energy gradient is the direction which points to the saddle point. Since the attempts are those which try to overcome the barrier between two energy minima via the saddle point, the lowest frequency of the energy oscillations in Fig. 1 is the frequency which enters the first equation noted in the abstract. Therefore, we find $\nu\approx1.5\times10^{12}$ Hz.

The distance between two minima, that is, the hopping distance l in the corundum structure is equal to 3.802 Å. These calculated values of l, ν, and E_a allow us to calculate the diffusion in α-Al_2O_3 from Eq. (1).

To calculate the diffusion in liquid alumina, we conducted three *ab initio* MD runs at three temperatures 2000, 3000, and 4000 K. The alumina structure was obtained by first melting the α-Al_2O_3 at a temperature of 9000 K, after which it was thermalized at 4000 K. Then a hydrogen atom was placed at a random position (but not too close to Al or O atoms). This configuration was then used as the initial one in the simulation of hydrogen in alumina. The system was equilibrated for 2000 time steps and then another 4000 time steps were used to derive the hydrogen trajectories and from them calculate the diffusion. The diffusion was calculated using the Einstein relation

$$\langle|r(t)-r(0)|^2\rangle=6Dt, \tag{3}$$

where $r(t)$ is the position of the particle at time t and D is the diffusion coefficient. Then, using the results at 3000 and 4000 K, we approximated the diffusion coefficient by Eq. (1).

As the result we obtained

$$D(T)=(8.71\times10^{-7}\ \mathrm{m^2/s})\exp(-0.91\ \mathrm{eV}/kT). \tag{4}$$

The calculated diffusion at 2000 K is in agreement with this equation. The movement of hydrogen in liquid alumina was further visualized,[33] which allowed to understand the

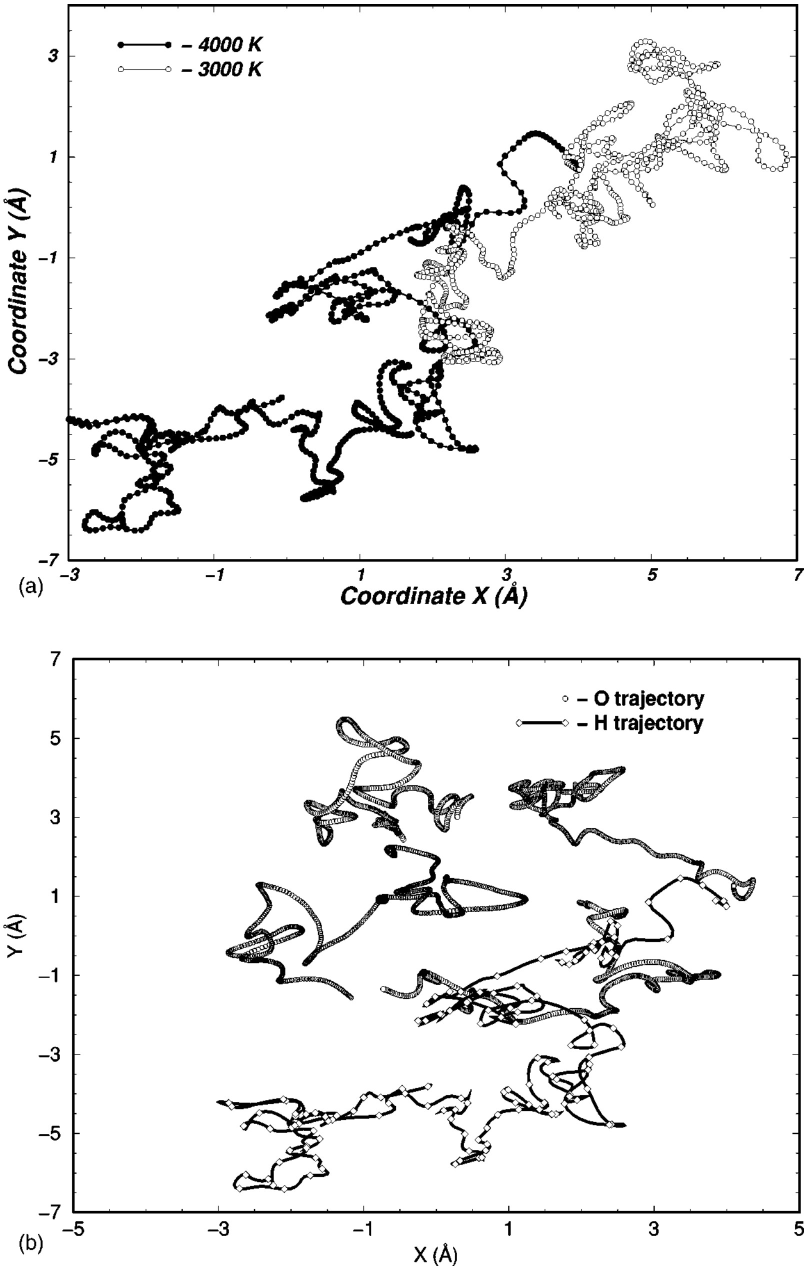

FIG. 2. Trajectories of (a) hydrogen calculated by *ab initio* MD in liquid Al_2O_3 at temperatures of 3000 K and 4000 K, (b) hydrogen and some oxygens calculated by *ab initio* MD in liquid Al_2O_3 at temperature of 4000 K.

mechanism of diffusion. The hydrogen atom is bonded to an O atom and moves with this oxygen, at the same time moving around its position. When two O atoms approach each other and the hydrogen atom is in between these two O atoms, the hydrogen atom might then jump from one O atom to the other and then move on with this atom. Figure 2(a) shows calculated trajectories of an hydrogen atom at 3000 K and 4000 K. The regions of trajectory densification correspond to periods when hydrogen performs motion around an O atom. The parts of trajectories which are comparatively straight[34,35] correspond to the jumps to neighboring O atoms. An O atom is heavy comparably to H and one can hardly expect the diffusion of O atoms to be as high as that of hydrogen. Figure 2(b) shows a comparison of O and H trajectories at a temperature of 4000 K. It is clear that the mobility of O atoms is low compared to the mobility of an H atom, therefore, the diffusion of H must occur not only by moving together with an adjacent O atom, but must also involve hopping of the H atom from one O atom to another.

Figure 3 demonstrates that the calculated mobility of H atoms is sufficiently converged. There is definitely some error which is difficult to estimate without performing additional much longer calculations which could provide us a statistics over jumps from one O atom to another. However, such long simulations are technically difficult. We note, that a typical simulation run takes about a few days running VASP in parallel on 32 fast CPU units.

A comparison of calculated and experimental data is shown in Fig. 4. The experimental data is obtained both for single crystal and polycrystalline α-Al_2O_3. Our calculations and experiments are in general agreement. There is a trend of the experimental diffusivity to increase faster with temperature than the calculated diffusivity in solid α-Al_2O_3. We can explain it by an increasing role of the diffusion via defects

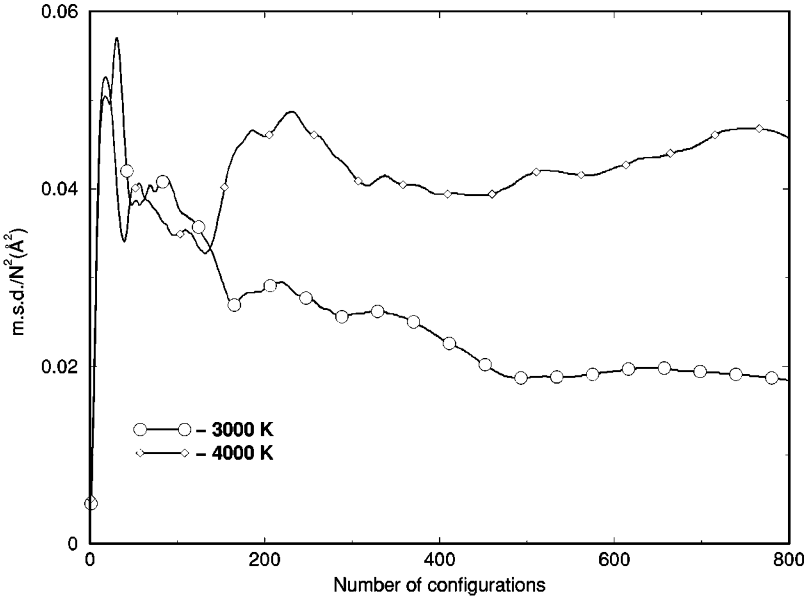

FIG. 3. Mean-square displacement averaged over N recorded configurations as a function of N at two different temperatures (see legend). The configurations are taken every 5th time step, where the time step is equal to 0.25 fs. The y axis shows $D \times \Delta t$, where D—diffusivity and Δt—time interval between configurations.

(such as a grain boundary, for example) with temperature. It is probable that the mechanism of hydrogen diffusion which we observe in liquid alumina is not valid at low temperature, because an O atom most likely has a very low mobility, and this, in turn, suppresses the mobility of hydrogen. However, when the temperature increases and the structure at a grain surface becomes increasingly more liquidlike, the diffusion of hydrogen probably occurs both via bulk as well as via liquidlike grain boundary structures. It is interesting to note that experimental diffusion at the highest temperature (Fig. 4) is practically identical to the diffusion calculated in liquid. This is a strong indication that the proposed mechanism and models of H diffusion in alumina might be valid.

IV. CONCLUSIONS

In this study, we performed first-principle static and dynamic calculations of diffusion of hydrogen in various forms of alumina. From as little information as the atomic numbers of the involved elements, we obtained data on diffusivity in good agreement with experiment. This suggests that our approximations for the mechanism of diffusion are realistic. Hydrogen diffusion occurs by hopping via saddle points between energy minima positions in corundum with preferential direction along the c axis. This direction might change when a H atom crosses a grain boundary at low temperature. However, when the temperature is high and the structure of a grain boundary is substantially different from that of corundum, diffusion is likely to occur via grain boundaries which is evidenced by the agreement between calculated and measured H diffusion in alumina. The diffusion of hydrogen in liquid alumina occurs via transfer of hydrogen from one oxygen to another. With increasing temperature both the "solid" and "liquid" mechanisms are likely to be relevant.

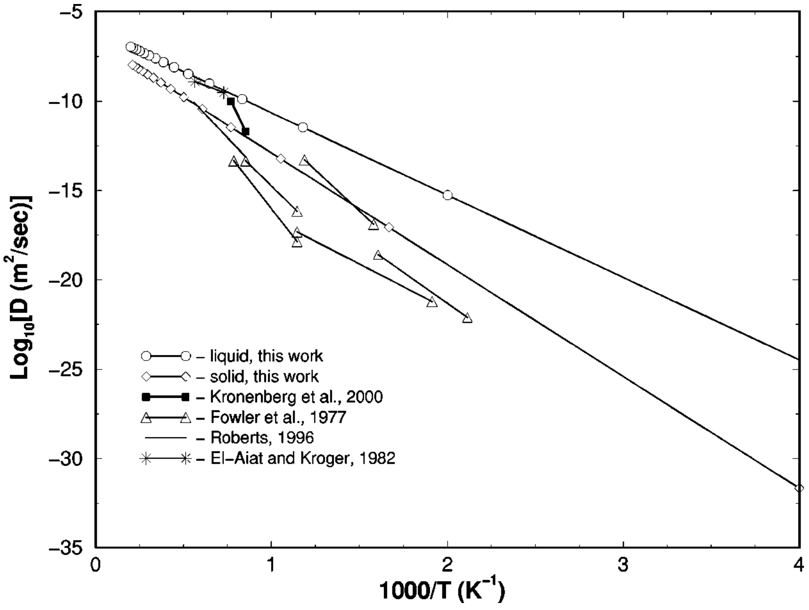

FIG. 4. Diffusivity of hydrogen in α and liquid alumina (in logarithmic units) compared to experimental data.

ACKNOWLEDGMENTS

A.B. is thankful to K. Refson for the Moldy software package. Discussions with B. Johansson are greatly appreciated. Computations are performed using the facilities of the National Supercomputer Center in Linköping. We also wish to thank the Swedish Foundation for Strategic Research (SSF) for financial support.

---

*Also at Applied Materials Physics, Department of Material Science and Engineering, The Royal Institute of Technology, SE-100 44 Stockholm, Sweden.

[1] J. Schott, in *Aquatic Chemical Kinetics*, edited by W. Stumm (Wiley, New York, 1990), p. 339.

[2] E. Protopopoff and P. Marcus, in *Corrosion Mechanisms in Theory and Practice*, edited by P. Marcus (Marcel Dekker, New York, 2002), p. 53.

[3] P. Kofstad, in *High Temperature Corrosion* (Elsevier Applied Science, London, 1988), p. 125.

[4] R. M. Roberts, in *Handbook of Gas Diffusion in Solids and Melts*, edited by J. E. Shelby (ASM International, USA, 1996), p. 84.

[5] M.M. El-Aiat and F.A. Kröger, J. Appl. Phys. **53**, 3658 (1982).

[6] G. Hultquist, B. Tveten, E. Hörnlund, M. Limbäck, and R. Haugsrud, Oxid. Met. **56**, 313 (2001).

[7] J. Oudar, in *Corrosion Mechanisms in Theory and Practice*, edited by P. Marcus (Marcel Dekker, New York, 2002), p. 19.

[8] I. Levin and D. Brandon, J. Am. Ceram. Soc. **81**, 1995 (1998).

[9] J. Skogsmo, M. Halvarsson, and S. Vourinen, Surf. Coat. Technol. **54-55**, 186 (1992).

[10] P. Hansson, M. Halvarsson, and S. Vourinen, Surf. Coat. Technol. **76-77**, 256 (1995).

[11] M.L. Kronberg, Acta Metall. **5**, 508 (1957).

[12] A.B. Belonoshko, Phys. Chem. Miner. **25**, 138 (1998).

[13] R. Ahuja, A.B. Belonoshko, and B. Johansson, Phys. Rev. E **57**, 1673 (1998).

[14] A.B. Belonoshko, R. Ahuja, and B. Johansson, Phys. Rev. B **61**, 3131 (2000).

[15] G. Gutiérrez, A.B. Belonoshko, R. Ahuja, and B. Johansson, Phys. Rev. E **61**, 2723 (2000).

[16] K.A. Johnson and N.W. Ashcroft, Nature (London) **403**, 632 (2000).

[17] M. Matsui, Miner. Mag. **58A**, 571 (1994).

[18] M. Matsui, Phys. Chem. Miner. **23**, 345 (1996).

[19] A.B. Belonoshko and S.K. Saxena, Geochim. Cosmochim. Acta **55**, 3191 (1991).

[20] G. Kresse and J. Hafner, Phys. Rev. B **47**, 558 (1993).

[21] G. Kresse and J. Hafner, Phys. Rev. B **49**, 14 251 (1994).

[22] G. Kresse and J. Furthmuller, Comput. Mater. Sci. **6**, 15 (1995).

[23] G. Kresse and J. Furthmuller, Phys. Rev. B **54**, 11 169 (1996).

[24] H.J. Monkhorst and J.D. Pack, Phys. Rev. B **13**, 5188 (1972).

[25] J.P. Perdew and Y. Wang, Phys. Rev. B **45**, 13 244 (1992).

[26] H. d'Amour, D. Schiferl, W. Denner, H. Schulz, and W.B. Holzapfel, J. Appl. Phys. **49**, 4411 (1978).

[27] P. Guenard, G. Renaud, A. Barbier, and M. Gautier-Soyer, Surf. Rev. Lett. **5**, 321 (1998).

[28] I. Batyrev, A. Alavi, and M.W. Finnis, Faraday Discuss. **114**, 33 (1999).

[29] M.A. San Miguel Barrera, J.F. Sanz, L.J. Alvarez, and J.A. Odriozola, Phys. Rev. B **58**, 6057 (1998).

[30] B. Tuttle, Phys. Rev. B **61**, 4417 (2000).

[31] M. Parrinello and A. Rahman, J. Appl. Phys. **52**, 7182 (1981).

[32] S. Nose, Mol. Phys. **52**, 255 (1984).

[33] See http://condmat.physics.kth.se/~anatoly/al2o3liq-h.mpg

[34] A.K. Kronenberg, J. Castaing, T.E. Mitchell, and S.H. Kirby, Acta Mater. **48**, 1481 (2000).

[35] J.D. Fowler, D. Chandra, T.S. Elleman, A.W. Payne, and K. Verghese, J. Am. Ceram. Soc. **60**, 155 (1977).